Research Article

A Ruthenium-Containing Organometallic Compound Reduces Tumor Growth through Induction of the Endoplasmic Reticulum Stress Gene *CHOP*

Xiangjun Meng,[1] Mili L. Leyva,[2] Marjorie Jenny,[1] Isabelle Gross,[6] Samir Benosman,[1] Bastien Fricker,[1] Sébastien Harlepp,[4] Pascal Hébraud,[4] Anne Boos,[5] Pauline Wlosik,[1] Pierre Bischoff,[3] Claude Sirlin,[2] Michel Pfeffer,[2] Jean-Philippe Loeffler,[1] and Christian Gaiddon[1]

[1]UMRS692 INSERM, Signalisations Moléculaires et Neurodégénérescence, Université de Strasbourg; [2]Institut de Chimie, UMR 7177 CNRS, Université de Strasbourg; [3]EA 3430, Centre Paul Strauss, Université de Strasbourg; [4]IPCMS, UMR 7504 CNRS; [5]UMR 7178 IPHC-DSA, UdS, CNRS, ECPM; and [6]UMRS682 INSERM, Université de Strasbourg, Strasbourg, France

Abstract

Cisplatin-derived anticancer therapy has been used for three decades despite its side effects. Other types of organometallic complexes, namely, some ruthenium-derived compounds (RDC), which would display cytotoxicity through different modes of action, might represent alternative therapeutic agents. We have studied both *in vitro* and *in vivo* the biological properties of RDC11, one of the most active compounds of a new class of RDCs that contain a covalent bond between the ruthenium atom and a carbon. We showed that RDC11 inhibited the growth of various tumors implanted in mice more efficiently than cisplatin. Importantly, in striking contrast with cisplatin, RDC11 did not cause severe side effects on the liver, kidneys, or the neuronal sensory system. We analyzed the mode of action of RDC11 and showed that RDC11 interacted poorly with DNA and induced only limited DNA damages compared with cisplatin, suggesting alternative transduction pathways. Indeed, we found that target genes of the endoplasmic reticulum stress pathway, such as *Bip, XBP1, PDI*, and *CHOP*, were activated in RDC11-treated cells. Induction of the transcription factor CHOP, a crucial mediator of endoplasmic reticulum stress apoptosis, was also confirmed in tumors treated with RDC11. Activation of CHOP led to the expression of several of its target genes, including proapoptotic genes. In addition, the silencing of *CHOP* by RNA interference significantly reduced the cytotoxicity of RDC11. Altogether, our results led us to conclude that RDC11 acts by an atypical pathway involving CHOP and endoplasmic reticulum stress, and thus might provide an interesting alternative for anticancer therapy. [Cancer Res 2009;69(13):5458–66]

Introduction

Various metal complexes have been tested in anticancer therapy (1–3). In particular, cisplatin has become one of the most widely used drugs and is highly effective in treating several cancers such as ovarian and testicular cancers (4). However, cisplatin displays, along with other kinds of anticancer drugs, two major drawbacks: (*a*) severe toxicities (neurotoxicity, nephrotoxicity, etc.) and (*b*) limited applicability to a narrow range of tumors, as several of them exhibit natural or induced resistance (4–6).

In the search of new therapies avoiding these drawbacks, other metals have been considered as alternatives to platinum. Special attention has been paid to ruthenium compounds because they exhibit cytotoxicity against cancer cells, analogous ligand-exchange abilities to platinum complexes, no cross-resistance with cisplatin, and may display reduced toxicity against healthy tissues by using iron transport (1–3, 7). One of the first ruthenium compounds described to have anticancer activity was ruthenium red (8), and further work showed the anticancer potential of ruthenium-containing drugs (9, 10). Since then, several teams have synthesized and characterized new compounds containing ruthenium (II) or ruthenium (III) (11–16). Two of these compounds, NAMI-A and KP109, have entered preclinical and/or clinical trials (17, 18).

Based on the similarities with platinum compounds (19), studies on the mode of action of ruthenium-containing compounds focused on their interaction with DNA (20–22). Indeed, several ruthenium-containing drugs interact with DNA and modify its structure, suggesting that they might induce DNA damages. Activation of p53 or p73 by some of these drugs partly corroborated this hypothesis (23–25). Alternative modes of action have also been described, including production of reactive oxygen species (26), inhibition of kinases (27), modification of enzymatic activities (28), or redox reactions (29). Obviously, the variety of these effects might be linked to the structural diversity of the ruthenium complexes.

Most of the ruthenium-containing compounds described have ligands that are relatively weakly bound to the metal via a heteroatom (N, O, S). In contrast, we have synthesized several ruthenium-based complexes in which the ligand is bound to the metal via strong covalent bonds such as a C-M ó bond (23, 30). The stability of this bond ensures the attachment of the ligand to the metal and enhances the biological activity of the complex. Besides, the electronic behavior of the ruthenium and thus its reactivity might be slightly different. We have called these molecules ruthenium-derived compounds (RDC) and previously showed that several RDCs are cytotoxic *in vitro* for several cancer cell lines that are sensitive or resistant to cisplatin (23). In the present study, we further characterized RDC11, one of the most active RDCs, by showing its *in vivo* properties and by investigating its mode of action independently of p53 proteins and DNA damages.
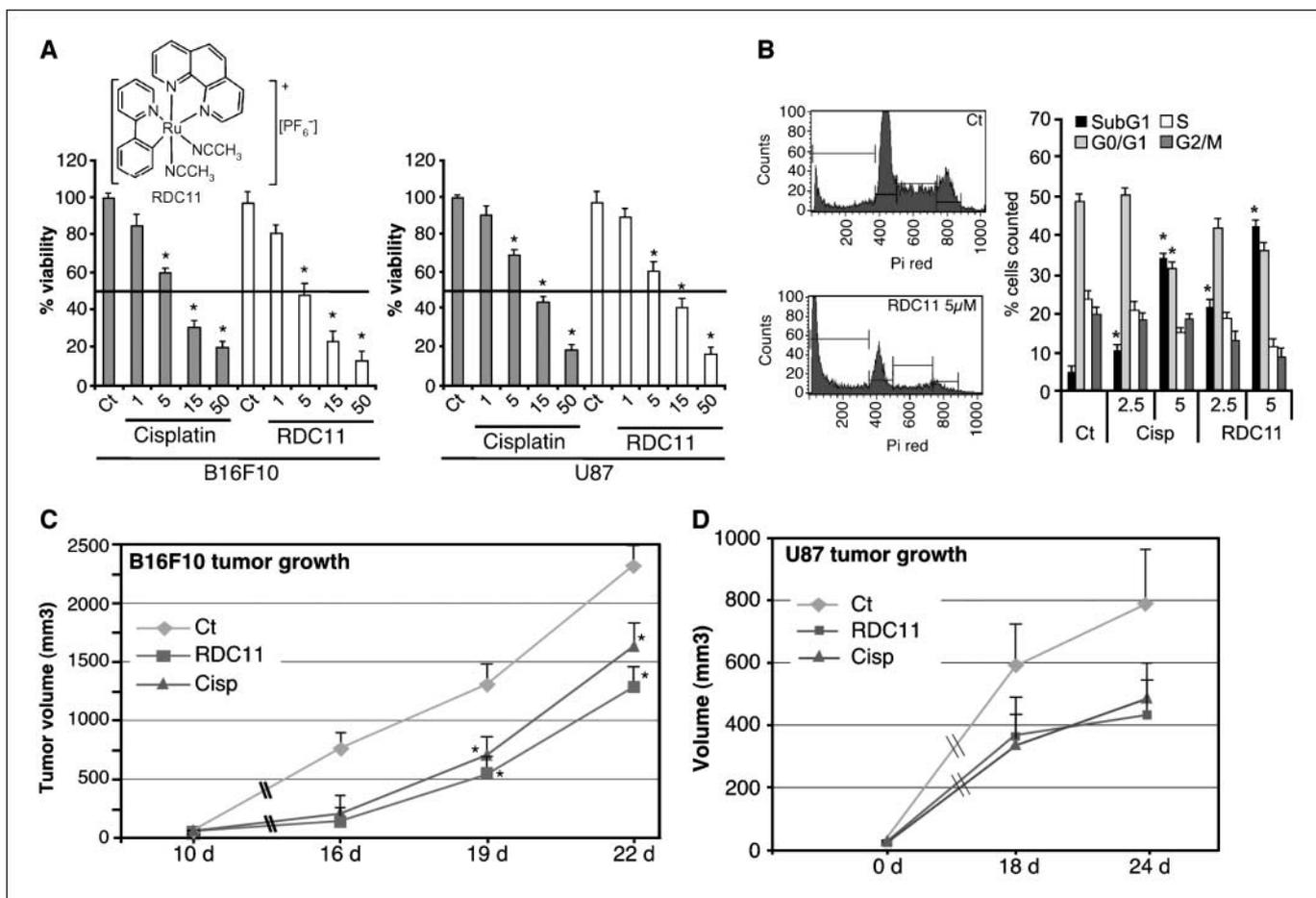
Fig. 1. RDC11 inhibits tumor growth *in vivo. A,* B16F10 mouse melanoma cells or U87 human glioblastoma cells were treated in 96-wells plates for 48 h with the indicated concentration (micromolar) of cisplatin or RDC11. Viability of the cells was evaluated using a MTT test. *Inset,* RDC11 structure. *B,* cell cycle profile analysis of B16F10 cells treated with cisplatin or RDC11 (2.5 or 5 μmol/L) for 48 h. Cells were stained with propidium iodide and analyzed by fluorescence-activated cell sorting. *Left,* graphs representing DNA content profile of control cells or cells treated with RDC11 (5 μmol/L). *Right, columns,* mean of three wells of a representative experiment; *bars,* SD. *C,* C57BL/6 mice (8 wk old) were injected s.c. with 5×10^5 B16F10 cells. Injections of equivalent doses of RDC11 or cisplatin (13.3 μmol/kg) were started when tumors were palpable (10 d after injection) and were done twice a week. Graph shows tumor volumes; representative of three independent experiments (*n* = 8). *D,* nude mice (Swiss nu/nu, Charles River; 8 wk old) were injected s.c. with 5×10^5 U87 cells. When tumors were palpable, injections of molar equivalent doses of RDC11 or cisplatin were done twice a week during 24 d. Graph represents tumor volumes; representative of three independent experiments (*n* = 8). *, *P* < 0.01, compared with control, as calculated by a one-way ANOVA test followed by a Newman-Keuls test over three independent experiments.

Materials and Methods

Cell culture, 3-(4,5-dimethylthiazol-2-yl)-2,5-diphenyltetrazolium bromide test, and flow cytometry analysis. B16F10, U87, and TK6 cells were obtained from American Type Culture Collection. NH32 cells were provided by Dr. H. Liber (Department of Radiation Oncology, University of Washington, Seattle, WA). Cells were maintained in DMEM with 10% fetal bovine serum and incubated in the presence of 5% CO_2/95% air at 37°C. 3-(4,5-Dimethylthiazol-2-yl)-2,5-diphenyltetrazolium bromide (MTT) tests were done with cells cultured in 96-well culture dishes (Costar) as previously described (31). Hypodiploid DNA was measured as described (32) using propidium iodide. The fluorescence of 10,000 cells was analyzed using a FACScan flow cytometer and CellQuest software (Becton Dickinson).

Western blot. Cells were treated in triplicates, lysed, and Western blots were done as described (31). Equal loading was verified with an actin antibody (1/200; Dr. Aunis, Physiopathologic du Systeme nerveux, INSERM U575, Strasbourg, France). Immunoprobing was done with anti-Bip (1/250; Santa Cruz Biotechnology), anti-XBP1 (1/250; Santa Cruz Biotechnology), anti–phospho-H2AX antibody (1/3,000; Millipore), anti-CHOP (1/1,000; Santa Cruz Biotechnology), or anti-p53 (421, supernatant 1/3) antibodies. Membranes were probed with a secondary horseradish peroxidase–conjugated antibody (antirabbit, antigoat, or antimouse) diluted at 1/2,000.

Quantitative real-time reverse transcription-PCR. Total RNA was extracted using RNAII Nucleospin (Macherey-Nagel). Reverse transcription was done with 1 μg RNA using Bio-Rad iScript kit. Quantitative PCR was done in Bio-Rad iCycler thermal cycler using iQ SYBR Green supermix (Bio-Rad Laboratories). Starting quantities of genes of interest were reported to those of a housekeeping gene (*18S*). Specificity of the amplification was controlled by a melting curve (31). Primer sequences are shown in Supplementary Materials and Methods.

siRNA silencing. CHOP siRNAs against human CHOP were purchased form Dharmacon (*DDIT* smart pool siRNA). SiRNAs were transfected in cells using Lipofectamine 2000 (Invitrogen) as described previously (33).

Blood biochemistry measures. C57BL/6 mice were treated chronically by i.p. injection twice a week (13.3 μmol/kg, solution PBS/Cremophore) over 3 wk. Animals were subjected to anesthesia and blood samples were taken. Biochemistry measurements were done at the Institut Clinique de la Souris (Strasbourg, France).

Luciferase assay. Luciferase assays were done as described (31). Luciferase activity was measured by a luminometer (Berthold systems). Normalization of luciferase activity was done by replacing the reporter gene of interest by a cytomegalovirus luciferase reporter vector. CHOP and TRB3 reporter plasmids were previously described (34–37).

Chromatin immunoprecipitation. Cells were fixed with 1% (v/v) formaldehyde for 10 min at room temperature and quenched with 0.125 mol/L glycine for 5 min. Chromatin immunoprecipitation experiments were carried out using the EZ-Magna ChIP Chromatin Immunoprecipitation Kit (Millipore). Sheared cross-linked chromatin from ∼10^6 cells was incubated overnight at 4°C with 3 μg of mouse anti-CHOP (Santa Cruz Biotechnology) or normal mouse IgG (Millipore). Input corresponds to nonimmunoprecipitated sheared cross-linked chromatin from ∼10^5 cells (1%). PCR analysis was done with 1/25th of immunoprecipitated DNA as template and primers of the mouse *Trb3* proximal promoter (forward, GGGCGTGTGGCCCCGAAG; reverse, GGATCCCCGCCCGGCTGAT).

Results

RDC11 inhibits the growth of various tumors implanted in mice. To test the efficiency of RDC11 *in vivo*, we chose to implant B16F10 mouse melanoma cells in C57BL/6 mice and to use the organometallic compound cisplatin as reference. We verified that RDC11 reduced B16F10 cell number *in vitro* with an IC$_{50}$ of 5 μmol/L, which was similar to the IC$_{50}$ of cisplatin (Fig. 1A). As previously shown for other RDCs (23), RDC11 favored the apparition of a sub-G$_1$ fraction in cell cycle profiles (Fig. 1B) and induced nuclear condensation, as well as caspase-3 activation (Supplementary Data 1A), showing that RDC11 induced cell death

in B16F10. Next, B16F10 cells were implanted s.c. in mice. When tumors were palpable, mice were injected i.p. twice a week for 2 weeks with equivalent molar doses of RDC11 or cisplatin (Fig. 1C). RDC11 reduced the volume (Fig. 1B) and weight of the tumors by 40% compared with the control (Supplementary Data #1B). Of note, the activity of RDC11 was better than that of cisplatin.

To further evaluate the activity of RDCs *in vivo*, we also used human glioblastoma cells. MTT tests showed that RDC11 reduced the number of glioblastoma cells with an IC$_{50}$ between 1 and 5 μmol/L, except for U87 cells (Fig. 1A; Supplementary Data #1C). Cell cycle profile analyses showed that RDC11 also induced the sub-G$_1$ phase in glioblastoma cells (Supplementary Data #1D). U87 cells were selected for *in vivo* studies in nude mice (Fig. 1D). Twenty-four days after implantation, RDC11- and cisplatin-injected mice had a tumor volume 45% smaller compared with control mice. A similar reduction of tumor size after RDC11 treatment was also observed on a model of xenografted A2780 ovarian cancer cells in nude mice (Supplementary Data #2A).

These results indicated that RDC11 was able to significantly decrease the growth of mouse and human tumors *in vivo*.

RDC11 leads to reduced chronic toxicity compared with cisplatin. One of the major drawbacks of chemotherapies is the lack of selectivity toward cancer cells, leading to side effects on several tissues, such as the kidneys or the sensory nervous
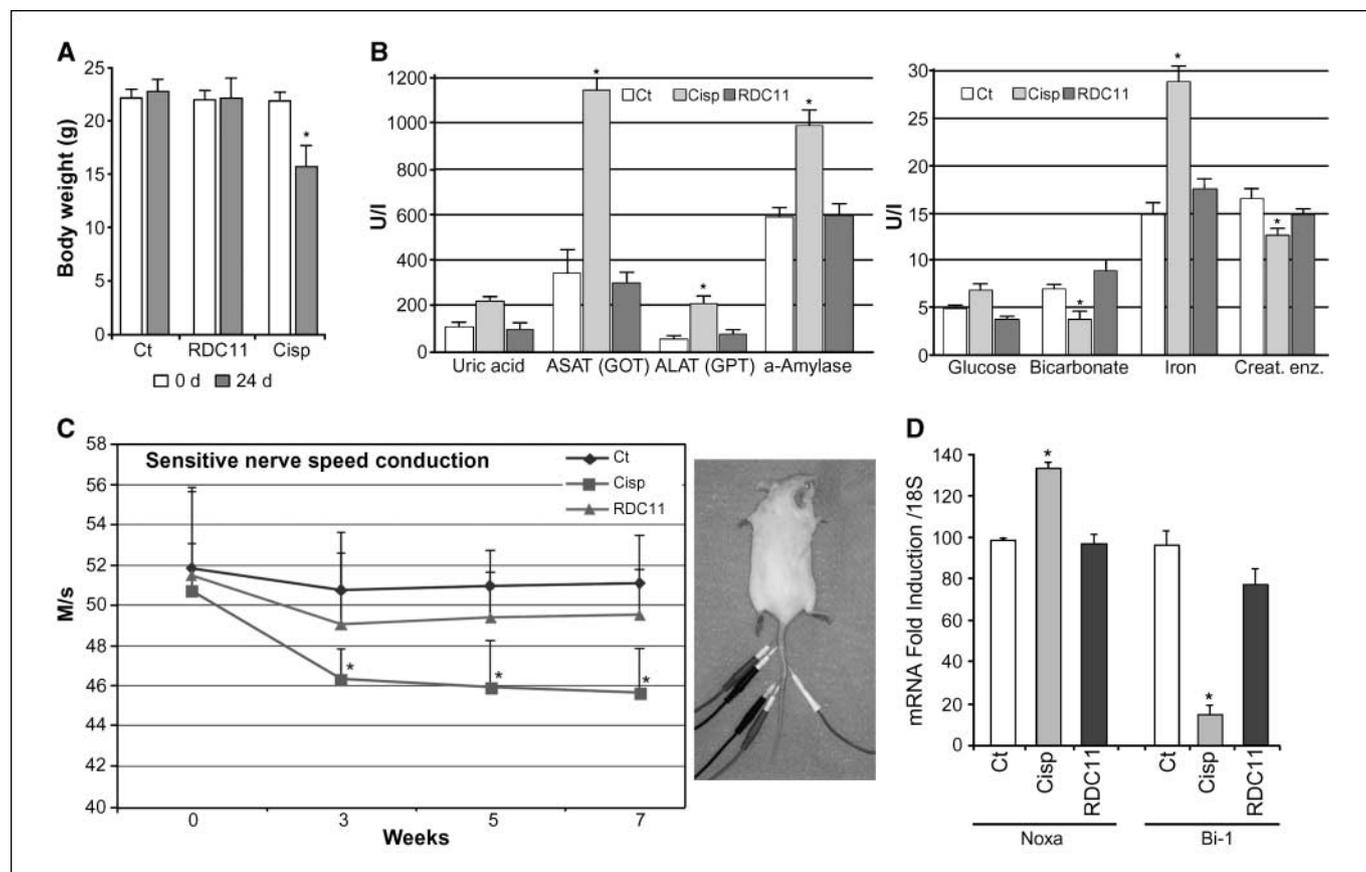

Fig. 2. Effects of RDC11 on healthy tissues. *A* to *D*, C57BL/6 mice (8 wk old) were injected repeatedly over 3 or 7 wk with RDC11 or cisplatin (13.3 μmol/kg) twice a week. *A*, graph represents weight of mice before and 24 d after the first injection. *B*, after 7 wk, blood samples were taken and markers for liver and kidney toxicity were analyzed. *C*, animals were also analyzed for sensory nerve conductance speed (Supplementary Materials and Methods). *Points,* mean conductance speed (*n* = 8); *bars,* SD. *Right,* montage used to measure electric properties of the tail sensory nerve. *D*, at the end of the protocol, animals were sacrificed and dorsal root ganglia were dissected out. Quantitative real-time reverse transcription-PCR (RT-qPCR) was done using primers for Noxa, Bi-1, and 18S mRNA. Data are represented as fold inductions relative to untreated cells (*Ct*) and were normalized with 18S levels. *Columns,* mean (*n* = 8); *bars,* SD. *, *P* < 0.01, compared with control (one-way ANOVA test followed by a Newman-Keuls test).
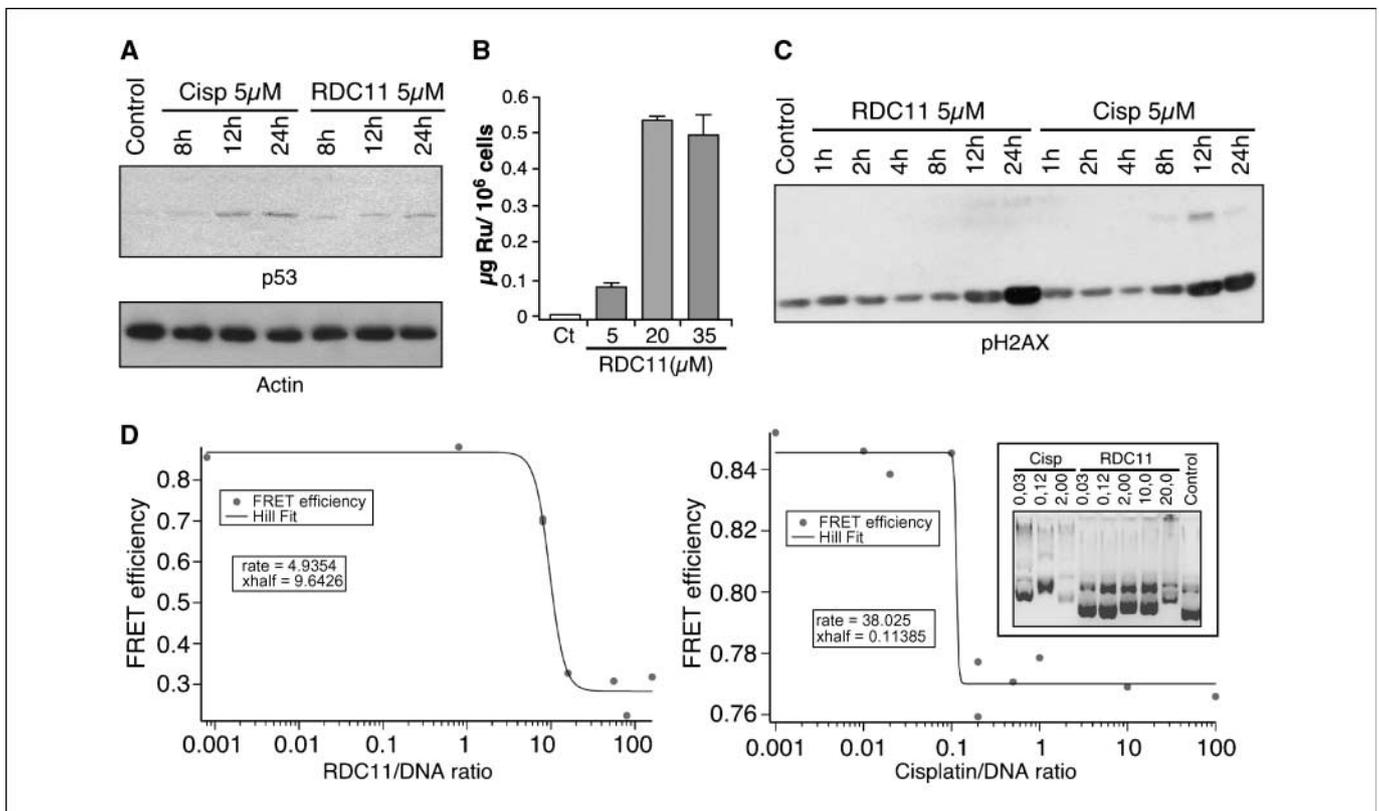
Fig. 3. Analyses of RDC11 interaction with DNA. *A* and *C,* Western blot analysis of cells treated for the indicated time with 5 μmol/L of cisplatin or RDC11. Immunoblotting was done with anti-p53, anti-actin, and anti–phospho-H2AX antibodies. *B,* graph represents the intracellular content of ruthenium in micrograms per 10^6 cells incubated for 24 h with different concentrations of RDC11. Intracellular ruthenium content was assessed using induced coupled plasma mass spectrometry (Supplementary Materials and Methods). *D,* efficiency of the FRET between the extremities of a 14-bp-long double-stranded DNA labeled with Alexa 488 and Alexa 568. The measurements were done at the equilibrium of complexation of DNA with the metal complex, after the addition of RDC11 (*left*) or cisplatin (*right*; Supplementary Materials and Methods). *Solid line,* fit of the experimental data with a Hill function $H(x) = base + A * 1/[1 + (xhalf/x)^{rate}]$. *Inset,* circular double-stranded DNA was incubated with cisplatin or RDC11 in the indicated ratio (DNA base pairs/molecule of drugs). Complexes were run on a 1% agarose gel to observe DNA relaxation.

system (5, 6). Therefore, we checked the deleterious effects induced by RDC11 in mice. In a single dose experiment, the LD_{50} was similar to cisplatin (∼57 μmol/kg; Supplementary Data #2*B*). To evaluate the chronic toxicity of RDC11, C57BL/6 mice were periodically injected with equivalent doses of RDC11 or cisplatin following the protocol described in Fig. 1*C*. After 3 weeks, cisplatin reduced body weights by about 25%, in contrast to RDC11, which had no significant effect (Fig. 2*A*). Biomedical analysis of blood markers showed that cisplatin induced variations in uric acid, aspartate aminotransferase, alanine aminotransferase, α-amylase, glucose, bicarbonate, and iron, corresponding to alterations in hepatic and renal functions (Fig. 2*B*). No significant changes were observed for these blood markers in RDC11-treated mice.

To analyze the toxicity on sensory nerves, we recorded their conduction using electromyography on C57BL/6 mice periodically injected as described above. Three weeks after the first injection, cisplatin significantly reduced the speed of sensory nerve conduction, whereas RDC11 affected it only modestly (Fig. 2*C*). A gene expression analysis in sensory neurons of dorsal root ganglia revealed that the proapoptotic gene *Noxa* was up-regulated by cisplatin, whereas the antiapoptotic gene *Bi-1* was inhibited (Fig. 2*D*; ref. 38). Interestingly, both genes were not significantly affected by RDC11 treatments. This reduced toxicity of RDC11 on healthy tissues can be correlated to the diminished cytotoxicity of

RDC11 on primary culture of glial cells compared with glioblastoma cells (Supplementary Data #2*C*).

RDC11 interacts with DNA and induces DNA damage *in vivo*. It is important to understand the mode of action of anticancer drugs to improve their design and their use in combinatory or tumor-selective treatments. Numerous studies indicated that ruthenium-derived compounds interact with DNA (20–22), which is consistent with our previous finding that RDCs induce p53 (23). RDC11 can also induce p53 protein levels (Fig. 3*A*) and p53 target genes (*p21, GADD45,* and *PUMA*; ref. 39; Supplementary Data #3*A*). However, we had previously shown that p53 was not absolutely necessary for RDC cytotoxicity (23), which is also the case for RDC11 (Supplementary Data #3*B*). Therefore, there was an unresolved question about whether RDCs interact with DNA and induce DNA damages.

We first verified that RDC11 entered the cells (Fig. 3*B*). Then, we followed the induction of DNA damages using as a marker the phosphorylation of histone H2AX at serine 137 (40). Treatment with cisplatin induced phosphorylation after 12 hours, whereas 24 hours were required for RDC11 (Fig. 3*C*). To evaluate whether RDC11 interacted with DNA, Förster resonance energy transfer (FRET) experiments were done using a double-stranded oligonucleotide labeled by two fluorophores at each end of one of the oligonucleotides (Fig. 3*D*). The ability of cisplatin and RDC11 to interact with the oligonucleotides was measured as a decrease of

the FRET efficiency, which is proportional to the separation of the fluorophores. The efficiency of the transfer decreased very rapidly at a critical drug concentration, corresponding at a molar ratio with DNA of 0.1 to 1 in the case of cisplatin and 10 to 1 in the case of RDC11. Calculations indicated that, at equilibrium, the length of the DNA increases by 15%, from 4.6 to 5 nm, when cisplatin is added, whereas it increases by 41%, up to 7.1 nm, when RDC11 is added. Therefore, both RDC11 and cisplatin induced a different structural change of the DNA double strand, and the affinity of cisplatin for DNA is 2 orders of magnitude higher than that of RDC11. The direct interaction and the lower affinity of RDC11 for DNA compared with cisplatin were confirmed by testing the ability of these drugs to relax a circular, double-stranded DNA using increasing ratios between the base pairs and the number of molecules of drug (Fig. 3D, *inset*).

The reduced ability of RDC11 to interact with DNA and the p53-independent activity of RDC suggested that alternative pathways might be involved in addition to the induction of DNA damages.

RDC11 induces the activity of components of the endoplasmic reticulum stress pathway. As an alternative mode of action for RDC11, we investigated the endoplasmic reticulum stress pathway, given that cisplatin was reported to regulate it (41). We examined the expression of typical endoplasmic reticulum stress–inducible genes (*Bip*, *XBP1*, and *PDI*; refs. 42, 43). As positive control, we treated the cells with tunicamycin. Interestingly, we found that RDC11 clearly stimulated these endoplasmic reticulum genes, which was not the case for cisplatin. We also confirmed the induction of *Bip* and *XBP1* by Western blot (Fig. 4B).

To further characterize the role of the endoplasmic reticulum stress pathway in RDC11 activity, we followed the expression of the transcription factor CHOP, which has been described as a critical mediator of endoplasmic reticulum stress apoptosis (44–46). We found that RDC11 significantly induced CHOP mRNA levels and
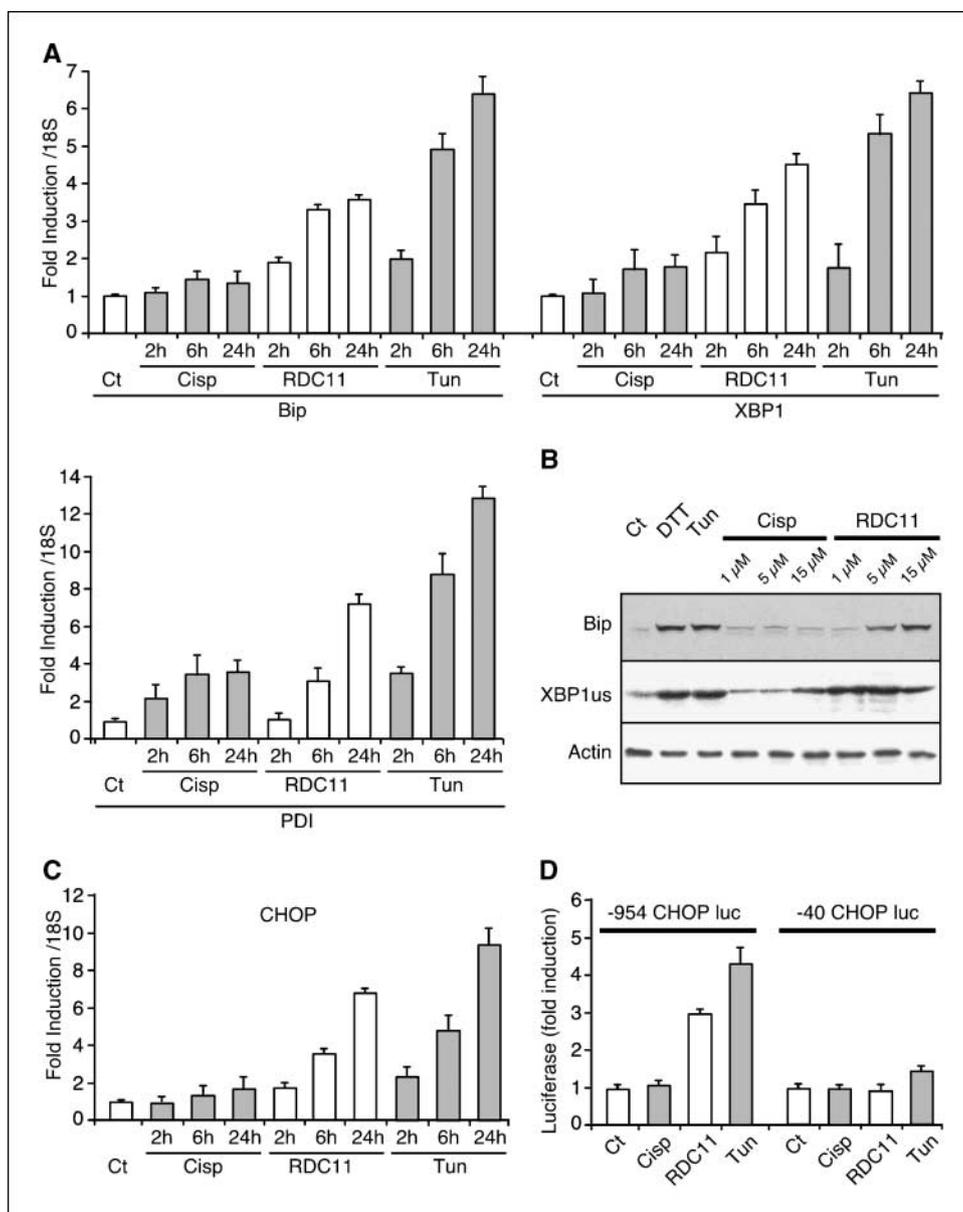

Fig. 4. RDC11 induces components of the endoplasmic reticulum stress pathway. *A* and *C*, B16F10 cells were treated with cisplatin (5 μmol/L), RDC11 (5 μmol/L), or tunicamycin (*Tun*; 10 μg/mL) for the indicated time (2, 6, and 24 h). RT-qPCR was done using primers for Bip, XBP1, PDI, CHOP, and 18S. Data are represented as fold inductions relative to untreated cells (*Ct*) and were normalized with 18S levels. *B*, B16F10 cells were treated with cisplatin, RDC11, tunicamycin (10 μg/mL), or DTT (1 mmol/L) for 24 h. Proteins were extracted and Western blot using anti-Bip, anti-XBP1 [unspliced (*us*)], and anti-actin antibodies was done. *D*, cells were cotransfected with a luciferase reporter gene containing either the full-length CHOP promoter (−954/+91) or a deletion variant (−40/+91). Cells were then treated with 5 μmol/L of RDC11 or cisplatin or 10 μg/mL tunicamycin for 24 h before luciferase assay. Results of a representative experiment are shown as fold induction compared with untreated cells. *Columns*, means of triplicates; *bars*, SD.

Fig. 5. RDC11 stimulates expression of CHOP. *A* and *B*, B16F10 cells were treated with 5 μmol/L of cisplatin or RDC11 or 10 μg/mL tunicamycin for the indicated time (*A*) or with the indicated concentrations for 24 h (*B*). Proteins were extracted and Western blot using CHOP, H2AX, or actin antibodies was done. *C*, C57BL/6 mice (8 wk old) were injected s.c. with 5×10^5 B16F10 cells. Three injections of equivalent doses of RDC11 or cisplatin (13.3 μmol/kg) were started when tumors were palpable (10 d after injection). Animals were sacrificed and proteins were extracted from tumors 6 or 24 h after the last injection. CHOP and actin expression was detected by Western blot. *D*, Western blot analysis of CHOP expression in p53$^{-/-}$ NH32 cells and the parental TK6 counterpart treated with cisplatin (5 μmol/L) and RDC11 (5 μmol/L). Proteins were extracted and Western blot using CHOP, p53, or actin antibodies was done.
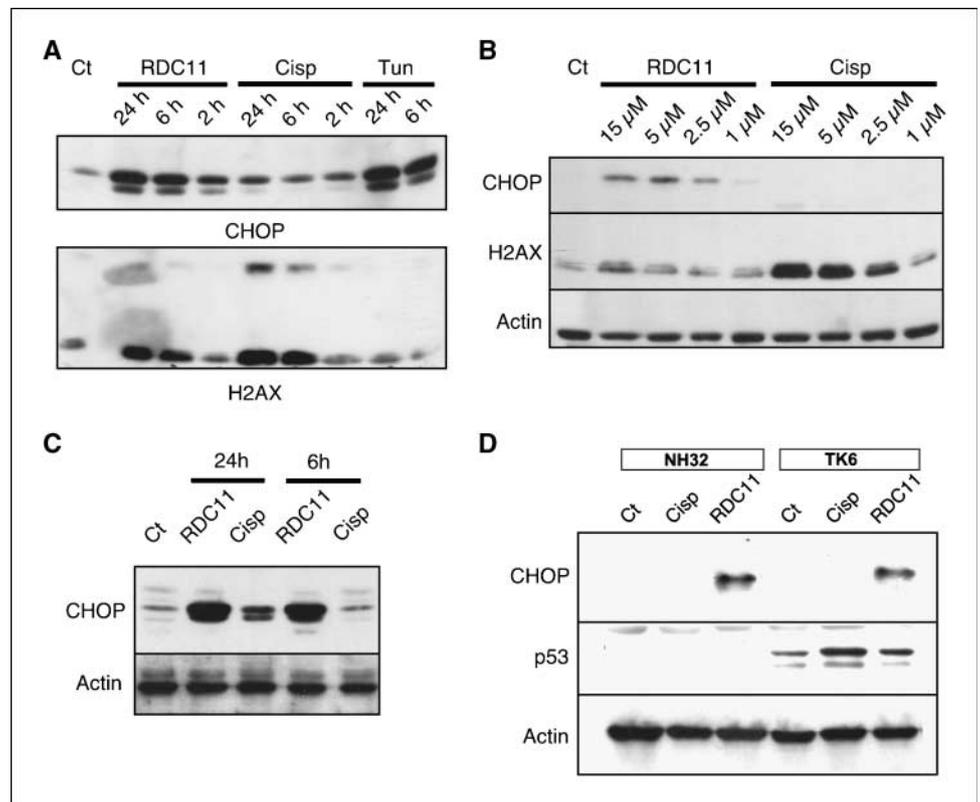
promoter activity (Fig. 4*C* and *D*; ref. 37). This induction was confirmed at the protein level *in vivo* (B16F10-derived tumors in C57BL/6 mice; Fig. 5*C*; Supplementary Data #4) and *in vitro* (B16F10 and U87 cells; Fig. 5*A–D*; Supplementary Data #3*C*). *In vitro*, the intensity of CHOP induction by RDC11 was similar to the one observed with tunicamycin, indicating that this induction was physiologically relevant. In all cases, cisplatin only marginally induced CHOP expression. RDC11 induced CHOP expression in a dose-dependent manner (Fig. 5*B*; Supplementary Data #3*C*). Note that the weak induction of CHOP expression at 1 μmol/L correlates with a limited action of RDC11 on cell viability, whereas a more robust induction of CHOP correlated with a more stringent effect of RDC11 (Fig. 1*A*). Interestingly, comparison of CHOP induction and phosphorylation of histone H2AX by different doses of RDC11 and cisplatin showed striking opposite effects: Cisplatin was more potent on H2AX phosphorylation, whereas RDC11 more significantly induced CHOP (Fig. 5*A* and *B*).

To assess whether the induction of CHOP was dependent of p53, we used the NH32 p53-knockdown cell line and its parental counterpart (TK6; Fig. 5*D*): The absence of p53 did not significantly affect the ability of RDC11 to induce CHOP, suggesting that the two mechanisms were independently activated.

We also verified the functionality of the induced CHOP. We first followed the expression of two proapoptotic CHOP target genes, *TRB3* (34, 35) and *CHAC1* (47). RDC11 induced the mRNA levels of both genes (Fig. 6*A*). Furthermore, using reporter gene assays, we found that RDC11 activated the *TRB3* promoter dependently on the CHOP responsive element (Fig. 6*B*). Finally, using chromatin immunoprecipitation experiments, we showed that RDC11 stimulated the binding of CHOP to the *TRB3* promoter (Fig. 6*C*; ref. 35).

To assess the importance of CHOP induction in RDC11 activity, we used validated siRNA directed against CHOP and analyzed if it would affect RDC11 activity in U87 cells. The siRNA directed against CHOP significantly reduced the expression of CHOP, whereas control and mutated siRNAs had no effect (Fig. 6*C, inset*). The silencing of CHOP expression significantly improved the viability of cells treated with various concentrations of RDC11, strongly suggesting that CHOP is necessary for RDC11 cytotoxicity (Fig. 6*D*). To further confirm the proapoptotic role of CHOP, we showed that overexpression of CHOP induced cell death and favored the biological activity of RDC11 (Supplementary Data #3*D*).

Discussion

Platinum-based therapies have been used for decades in anticancer protocols despite their limitations, such as resistance of certain types of cancers or secondary effects. To fill these gaps, we have recently characterized the biological activities of a new class of organometallic drugs containing a ruthenium atom. The stability of these compounds is increased, and we have previously shown that they exhibited a strong cytotoxicity *in vitro* (23, 30). In this new study, we further characterized the properties of RDC11, one of our most efficient RDCs.

RDC11 reduces tumor growth *in vivo* with less toxicity. In this study, we have established, using three different *in vivo* models (B16F10, melanomas; U87, glioblastomas; A2780, ovarian cancer), that RDC11 has interesting anticancer activity (Fig. 1*C* and *D*; Supplementary Data #2*A*). Indeed, the comparison of RDC11 with cisplatin indicated that RDC11 has a slightly better activity on tumor growth but, more importantly, does not induce as much deleterious side effects such as weight loss, neurotoxicity,

nephrotoxicity, or liver toxicity (Fig. 2A–D). Nevertheless, as expected for cytotoxic compounds, overdose of RDC11 caused lethality at doses similar to cisplatin (Supplementary Data #2B).

Similarly to other RDCs (23), the anticancer activity of RDC11 can be explained by its ability to trigger cell death because it induced a sub-G_1 phase, the condensation of nuclei, and the activation of caspase-3 (Fig. 1B; Supplementary Data #1A and D), as we previously showed for other RDCs (23). However, cell cycle arrest can also be a part of the RDC11-driven effect, depending on the cell line and the concentration applied (23).

The lower toxicity of RDC11 chronic treatment was also supported by the reduced cytotoxicity of RDC11 on primary culture of glial cells compared with transformed cells (Supplementary Data #2C), which correlated with a reduced induction of CHOP protein levels in nonmalignant glial cells (Supplementary Data #3C). As proposed for other ruthenium-derived compounds, the lower toxicity of RDC11 might be attributed to its ability to mimic iron and the use of iron detoxification routes in the body or the differential cellular intake of iron between normal and cancer cells (1–3, 7).

RDC11 induces DNA damages. To understand more thoroughly the anticancer properties of RDC11, we have investigated its mode of action. We have shown in this study that RDC11 can enter the cell, interact with DNA, and provoke DNA damages (Fig. 3B–D). These properties explain the activation of p53 and its target genes (Fig. 3A; Supplementary Data #3A; ref. 23). However, our study also showed that RDC11 induces less DNA damages than cisplatin, which correlates with its lower affinity to DNA (Fig. 3C and D). These observations suggest that the contribution of DNA damage–activated pathways might not be critical for

RDC11 cytotoxicity, which is supported by the fact that the absence of p53 does not significantly impede RDC activity (Supplementary Data #3B; ref. 23).

However, even if this mode of action through DNA interaction seems less important compared with cisplatin, it has to be taken into account and is likely involved in RDC11 cytotoxicity. Indeed, the relative insensibility toward p53 deletion does not necessary mean that RDC11-induced DNA damages are not a significant part of the RDC11 proapoptotic mechanisms. For instance, RDC11 might induce DNA damage–dependent mechanisms through p53 homologues (p73; ref. 48) or other factors such as promyelocytic leukemia protein (49). The fact that overexpression of the dominant-negative isoform ΔNp73β reduced RDC11-induced cell death supports the possibility that p53 family members are involved in RDC11-induced cell death (Supplementary Data #3D; ref. 23). The induction by RDC11 of proapoptotic p53 target genes, such as *GADD45* and *Noxa*, can account for RDC11-induced cell death (39). Furthermore, we also observed an induction of genes involved in DNA damage repairs, such as *MDC1, HUS1*, and *RAD9* (data not shown; ref. 50).

RDC11 has multiple cellular targets, implicating the endoplasmic reticulum stress effector CHOP. The lack of strict correlation between the dramatic deleterious effect of RDC11 and its weak induction of DNA damages when compared with cisplatin (Figs. 1 and 3) suggested that RDC11 might have other cellular targets. We have now shown that RDC11 induced the expression of several genes of the endoplasmic reticulum stress pathway (*Bip, XBP1, PDI*, and *CHOP*; refs. 42, 43, 45, 46; Fig. 4), which represents the first report of a regulation of this pathway by a ruthenium-containing compound. Among these genes, we identified *CHOP* as
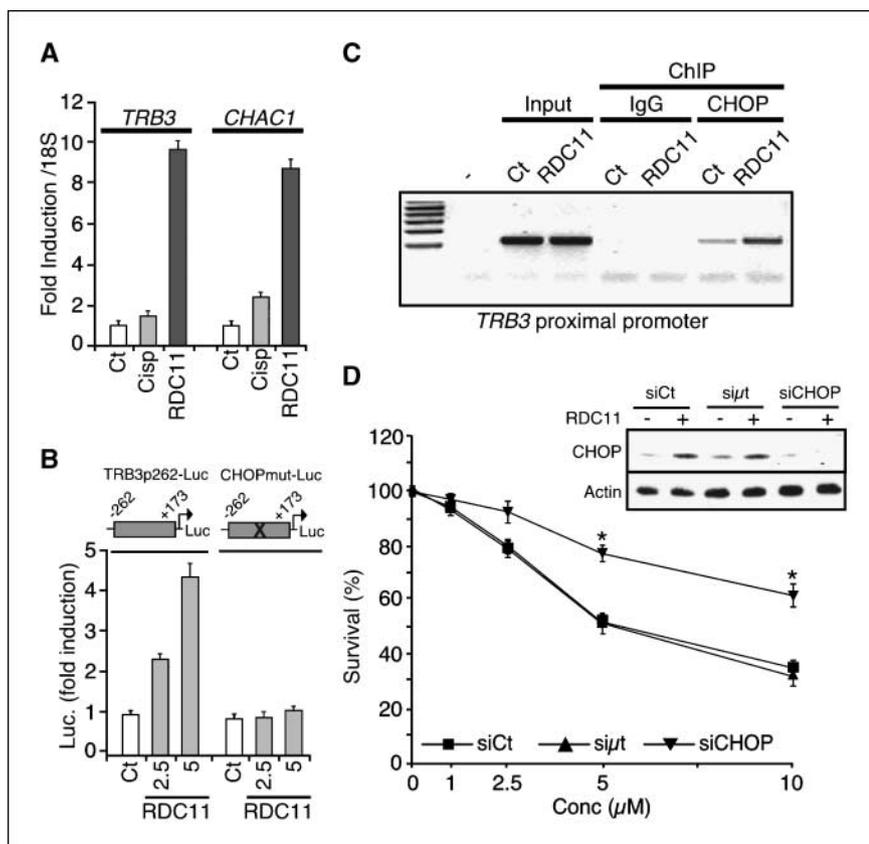

Fig. 6. CHOP activity is induced by RDC11 and is important for RDC11 effect. *A,* RDC11 induced the mRNA levels of *Trb3* and *CHAC1*. Cells were treated with cisplatin or RDC11 (5 μmol/L). RT-qPCR was done using primers for *Trb3, CHAC1,* and *18S*. Data are represented as fold inductions relative to untreated cells (*Ct*) and were normalized with 18S levels. *B,* RDC11 induced *TRB3* promoter through the CHOP responsive element. Cells were cotransfected with a luciferase reporter gene containing either the *Trb3* promoter (−262/+173) or a variant mutated in the CHOP binding site (*CHOPmut-Luc*). Cells were then treated with RDC11 (2.5 and 5 μmol/L) for 24 h before the luciferase assay. *C,* chromatin immunoprecipitation of CHOP on the proximal promoter of *Trb3*. Control or RDC11-treated (24 h, 5 μmol/L) B16F10 cell lysates were used for chromatin immunoprecipitation with control (normal mouse IgG) or CHOP antibodies. Agarose gel showing PCR amplification (35 cycles) of the *Trb3* proximal promoter using inputs (1% of chromatin used for chromatin immunoprecipitation) or ChIPs as templates. −, no template. *D,* U87 cells were transfected for 36 h with control siRNA (*Ct*), mutated CHOP siRNA, or siRNA directed against CHOP, before treatment with RDC11 for 48 h. Inset, CHOP expression was detected by Western blot. The graph corresponds to a MTT test done to detect cell viability at the indicated concentrations of RDC11.

functionally important for RDC11 cytotoxicity. First, we showed that RDC11 induced CHOP expression at the promoter level, leading to increased CHOP mRNA and protein levels *in vitro* and *in vivo* (Figs. 4C and D and 5A–D; Supplementary Data #4). Second, we showed that the elevated CHOP protein levels led to an increase in CHOP-dependent transcriptional activity, as (*a*) RDC11 treatment stimulated the expression of two CHOP proapoptotic target genes, *TRB3* and *CHAC1* (Fig. 6A), and (*b*) RDC11 induced the *TRB3* promoter activity through the binding of CHOP to this promoter (Fig. 6B and C). Finally, the silencing of CHOP significantly reduced the cytotoxicity of RDC11 (Fig. 6C), whereas on the contrary, CHOP overexpression facilitated RDC11-induced cell death (Supplementary Data #3D). This proapoptotic role of CHOP is in accord with the literature (43, 45, 46).

Altogether, our data suggest that RDCs activity involves at least two pathways: the DNA damage/p53 and the endoplasmic reticulum stress/CHOP pathways. It is rather difficult to precisely understand to what extent they are independently activated by RDC11 and if they act synergistically. However, three observations suggest that RDC11 might induce them independently. First, there was a clear discrimination between the induction of DNA damages and CHOP depending on the drugs used. RDC11 is less efficient in inducing DNA damage signaling (H2AX phosphorylation) but can strongly up-regulate CHOP expression (Figs. 3–5), whereas cisplatin, which induces much more important DNA damages, does not significantly regulate CHOP expression. The second argument is that the knockdown of p53 does not inhibit the expression of CHOP. Finally, a variant of RDC11 (RDC34), which displays a stronger affinity for DNA *in vitro*, does not exhibit a significant increase in its ability to induce CHOP expression (data

not shown). Because both pathways are activated by RDC11, it is likely that they both participate and might cooperate to allow a full cellular response to RDC11 treatment. The fact that both the silencing of CHOP and the inactivation of p53-like activity by ΔNp73β overexpression can reduce RDC11 activity supports this hypothesis. However, we do not exclude that other pathways might be also involved.

The ability of RDC11 to induce multiple and independent stress response pathways represents an interesting property for anticancer drugs that might allow a broader spectrum of action. It might also partly explain why RDCs are less sensitive toward cisplatin resistance mechanisms (23). In this aspect, the utilization and/or the targeting of this endoplasmic reticulum stress pathway in the future might enhance the spectrum of action and the efficiency of anticancer chemotherapy, as well as create new possibilities for effective combinatory treatments.

Disclosure of Potential Conflicts of Interest

No potential conflicts of interest were disclosed.

Acknowledgments

References

1. Bruijnincx PC, Sadler PJ. New trends for metal complexes with anticancer activity. Curr Opin Chem Biol 2008;12:197–206.
2. Jakupec MA, Galanski M, Arion VB, Hartinger CG, Keppler BK. Antitumour metal compounds: more than theme and variations. Dalton Trans 2008:183–94.
3. Dyson PJ, Sava G. Metal-based antitumour drugs in the post genomic era. Dalton Trans 2006:1929–33.
4. Kelland L. The resurgence of platinum-based cancer chemotherapy. Nat Rev Cancer 2007;7:573–84.
5. Kannarkat G, Lasher EE, Schiff D. Neurologic complications of chemotherapy agents. Curr Opin Neurol 2007;20:719–25.
6. Markman M. Toxicities of the platinum antineoplastic agents. Expert Opin Drug Saf 2003;2:597–607.
7. Allardyce CS, Dyson PJ. Ruthenium in medicine: current clinical uses and future prospects. Platinum Metals Rev 2001;45:62.
8. Anghileri LJ. The *in vivo* inhibition of tumor growth by ruthenium red: its relationship with the metabolism of calcium in the tumor. Z Krebsforsch Klin Onkol Cancer Res Clin Oncol 1975;83:213–7.
9. Giraldi T, Sava G, Bertoli G, Mestroni G, Zassinovich G. Antitumor action of two rhodium and ruthenium complexes in comparison with *cis*-diamminedichloroplatinum(II). Cancer Res 1977;37:2662–6.
10. Sava G, Giraldi T, Mestroni G, Zassinovich G. Antitumor effects of rhodium(I), iridium(I) and ruthenium(II) complexes in comparison with *cis*-dichlorodiammino platinum(II) in mice bearing Lewis lung carcinoma. Chem Biol Interact 1983;45:1–6.
11. Keppler BK, Balzer W, Seifried V. Synthesis and antitumor activity of triazolium-bis(triazole)-tetrachlororuthenate (III) and bistriazolium-triazolepentachlororuthenate (III). Two representatives of a new class of

inorganic antitumor agents. Arzneimittelforschung 1987;37:770–1.
12. Sava G, Pacor S, Zorzet S, Alessio E, Mestroni G. Antitumour properties of dimethylsulphoxide ruthenium (II) complexes in the Lewis lung carcinoma system. Pharmacol Res 1989;21:617–28.
13. Fruhauf S, Zeller WJ. New platinum, titanium, and ruthenium complexes with different patterns of DNA damage in rat ovarian tumor cells. Cancer Res 1991;51:2943–8.
14. Novakova O, Kasparkova J, Vrana O, van Vliet PM, Reedijk J, Brabec V. Correlation between cytotoxicity and DNA binding of polypyridyl ruthenium complexes. Biochemistry 1995;34:12369–78.
15. Morris RE, Aird RE, Murdoch Pdel S, et al. Inhibition of cancer cell growth by ruthenium(II) arene complexes. J Med Chem 2001;44:3616–21.
16. Scolaro C, Bergamo A, Brescacin L, et al. *In vitro* and *in vivo* evaluation of ruthenium(II)-arene PTA complexes. J Med Chem 2005;48:4161–71.
17. Depenbrock H, Schmelcher S, Peter R, et al. Preclinical activity of *trans*-indazolium[tetrachlorobisindazoleruthenate(III)] (NSC 666158; IndCR; KP 1019) against tumour colony-forming units and haematopoietic progenitor cells. Eur J Cancer 1997;33:2404–10.
18. Bergamo A, Gava B, Alessio E, et al. Ruthenium-based NAMI-A type complexes with *in vivo* selective metastasis reduction and *in vitro* invasion inhibition unrelated to cell cytotoxicity. Int J Oncol 2002;21:1331–8.
19. Cohen GL, Bauer WR, Barton JK, Lippard SJ. Binding of *cis*- and *trans*-dichlorodiammineplatinum(II) to DNA: evidence for unwinding and shortening of the double helix. Science 1979;203:1014–6.
20. Mei HY, Barton JK. Tris(tetramethylphenanthroline) ruthenium(II): a chiral probe that cleaves A-DNA conformations. Proc Natl Acad Sci U S A 1988;85:1339–43.
21. Brabec V. DNA modifications by antitumour platinum

and ruthenium compounds: their recognition and repair. Prog Nucleic Acid Res Mol Biol 2002;71:1–68.
22. Zeglis BM, Pierre VC, Barton JK. Metallo-intercalators and metallo-insertors. Chem Commun (Camb) 2007:4565–79.
23. Gaiddon C, Jeannequin P, Bischoff P, Pfeffer M, Sirlin C, Loeffler JP. Ruthenium (II)-derived organometallic compounds induce cytostatic and cytotoxic effects on mammalian cancer cell lines through p53-dependent and p53-independent mechanisms. J Pharmacol Exp Ther 2005;315:1403–11.
24. Hayward RL, Schornagel QC, Tente R, et al. Investigation of the role of Bax, p21/Waf1 and p53 as determinants of cellular responses in HCT116 colorectal cancer cells exposed to the novel cytotoxic ruthenium(II) organometallic agent, RM175. Cancer Chemother Pharmacol 2005;55:577–83.
25. Chatterjee S, Kundu S, Bhattacharyya A, Hartinger CG, Dyson PJ. The ruthenium(II)-arene compound RAPTA-C induces apoptosis in EAC cells through mitochondrial and p53-JNK pathways. J Biol Inorg Chem 2008;13:1149–55.
26. Jakupec MA, Reisner E, Eichinger A, et al. Redox-active antineoplastic ruthenium complexes with indazole: correlation of *in vitro* potency and reduction potential. J Med Chem 2005;48:2831–7.
27. Smalley KS, Contractor R, Haass NK, et al. An organometallic protein kinase inhibitor pharmacologically activates p53 and induces apoptosis in human melanoma cells. Cancer Res 2007;67:209–17.
28. Ang WH, De Luca A, Chapuis-Bernasconi C, Juillerat-Jeanneret L, Lo Bello M, Dyson PJ. Organometallic ruthenium inhibitors of glutathione-*S*-transferase P1-1 as anticancer drugs. ChemMedChem 2007.
29. Dougan SJ, Habtemariam A, McHale SE, Parsons S, Sadler PJ. Catalytic organometallic anticancer complexes. Proc Natl Acad Sci U S A 2008;105:11628–33.

Cancer Research

30. Leyva L, Sirlin C, Rubio L, et al. Synthesis of cycloruthenated compounds as potential anticancer agents. Eur J Inorg Chem 2007:3055–66.

31. Benosman S, Gross I, Clarke N, et al. Multiple neurotoxic stresses converge on MDMX proteolysis to cause neuronal apoptosis. Cell Death Differ 2007.

32. Nicoletti I, Migliorati G, Pagliacci MC, Grignani F, Riccardi C. A rapid and simple method for measuring thymocyte apoptosis by propidium iodide staining and flow cytometry. J Immunol Methods 1991;139: 271–9.

33. Gross I, Armant O, Benosman S, et al. Sprouty2 inhibits BDNF-induced signaling and modulates neuronal differentiation and survival. Cell Death Differ 2007; 14:1802–12.

34. Ord D, Ord T. Characterization of human NIPK (TRB3, SKIP3) gene activation in stressful conditions. Biochem Biophys Res Commun 2005;330:210–8.

35. Selim E, Frkanec JT, Cunard R. Fibrates upregulate TRB3 in lymphocytes independent of PPARα by augmenting CCAAT/enhancer-binding protein β (C/EBPβ) expression. Mol Immunol 2007;44:1218–29.

36. Ubeda M, Habener JF. CHOP transcription factor phosphorylation by casein kinase 2 inhibits transcriptional activation. J Biol Chem 2003;278:40514–20.

37. Bruhat A, Jousse C, Carraro V, Reimold AM, Ferrara M, Fafournoux P. Amino acids control mammalian gene transcription: activating transcription factor 2 is essential for the amino acid responsiveness of the CHOP promoter. Mol Cell Biol 2000;20:7192–204.

38. Reimers K, Choi CY, Bucan V, Vogt PM. The Bax Inhibitor-1 (BI-1) family in apoptosis and tumorigenesis. Curr Mol Med 2008;8:148–56.

39. Pietsch EC, Sykes SM, McMahon SB, Murphy ME. The p53 family and programmed cell death. Oncogene 2008; 27:6507–21.

40. Thiriet C, Hayes JJ. Chromatin in need of a fix: phosphorylation of H2AX connects chromatin to DNA repair. Mol Cell 2005;18:617–22.

41. Mandic A, Hansson J, Linder S, Shoshan MC. Cisplatin induces endoplasmic reticulum stress and nucleus-independent apoptotic signaling. J Biol Chem 2003;278:9100–6.

42. Shen J, Chen X, Hendershot L, Prywes R. ER stress regulation of ATF6 localization by dissociation of BiP/GRP78 binding and unmasking of Golgi localization signals. Dev Cell 2002;3:99–111.

43. Ron D, Walter P. Signal integration in the endoplasmic reticulum unfolded protein response. Nat Rev Mol Cell Biol 2007;8:519–29.

44. Marciniak SJ, Yun CY, Oyadomari S, et al. CHOP induces death by promoting protein synthesis and oxidation in the stressed endoplasmic reticulum. Genes Dev 2004;18:3066–77.

45. Zinszner H, Kuroda M, Wang X, et al. CHOP is implicated in programmed cell death in response to impaired function of the endoplasmic reticulum. Genes Dev 1998;12:982–95.

46. Oyadomari S, Mori M. Roles of CHOP/GADD153 in endoplasmic reticulum stress. Cell Death Differ 2004;11: 381–9.

47. Mungrue IN, Pagnon J, Kohannim O, Gargalovic PS, Lusis AJ. CHAC1/MGC4504 is a novel proapoptotic component of the unfolded protein response, downstream of the ATF4-3-CHOP cascade. J Immunol 2009;182:466–76.

48. Gong JG, Costanzo A, Yang HQ, et al. The tyrosine kinase c-Abl regulates p73 in apoptotic response to cisplatin-induced DNA damage [see comments]. Nature 1999;399:806–9.

49. Yang S, Kuo C, Bisi JE, Kim MK. PML-dependent apoptosis after DNA damage is regulated by the checkpoint kinase hCds1/Chk2. Nat Cell Biol 2002;4: 865–70.

50. Norbury CJ, Zhivotovsky B. DNA damage-induced apoptosis. Oncogene 2004;23:2797–808.

A Ruthenium-Containing Organometallic Compound Reduces Tumor Growth through Induction of the Endoplasmic Reticulum Stress Gene *CHOP*

Xiangjun Meng, Mili L. Leyva, Marjorie Jenny, et al.

Updated version	Access the most recent version of this article at: doi:10.1158/0008-5472.CAN-08-4408
Supplementary Material	Access the most recent supplemental material at: http://cancerres.aacrjournals.org/content/suppl/2009/06/12/0008-5472.CAN-08-4408.DC1

Cited articles	This article cites 44 articles, 13 of which you can access for free at: http://cancerres.aacrjournals.org/content/69/13/5458.full#ref-list-1
Citing articles	This article has been cited by 3 HighWire-hosted articles. Access the articles at: http://cancerres.aacrjournals.org/content/69/13/5458.full#related-urls

E-mail alerts	Sign up to receive free email-alerts related to this article or journal.
Reprints and Subscriptions	To order reprints of this article or to subscribe to the journal, contact the AACR Publications Department at pubs@aacr.org.
Permissions	To request permission to re-use all or part of this article, use this link http://cancerres.aacrjournals.org/content/69/13/5458. Click on "Request Permissions" which will take you to the Copyright Clearance Center's (CCC) Rightslink site.